**RAA 2016** Vol. **16** No. **4**, 69 (12pp) doi: 10.1088/1674–4527/16/4/069
*http://www.raa-journal.org* *http://iopscience.iop.org/raa*

***R**esearch in*
***A**stronomy and*
***A**strophysics*

# South Galactic Cap $u$-band Sky Survey (SCUSS): Project Overview

Xu Zhou[1], Xiao-Hui Fan[2], Zhou Fan[1], Bo-Liang He[1], Lin-Hua Jiang[5], Zhao-Ji Jiang[1], Yi-Peng Jing[3], Michael Lesser[2], Jun Ma[1], Jun-Dan Nie[1], Shi-Yin Shen[4], Jia-Li Wang[1], Zhen-Yu Wu[1], Tian-Meng Zhang[1], Zhi-Min Zhou[1] and Hu Zou[1]

[1] Key Laboratory of Optical Astronomy, National Astronomical Observatories, Chinese Academy of Sciences, Beijing 100012, China; *zhouxu@bao.ac.cn*
[2] Steward Observatory, University of Arizona, Tucson, AZ 85721, USA
[3] Center for Astronomy and Astrophysics, Department of Physics and Astronomy, Shanghai Jiao Tong University, Shanghai 200240, China
[4] Shanghai Astronomical Observatory, Chinese Academy of Sciences, Shanghai 200030, China
[5] Kavli Institute for Astronomy and Astrophysics, Peking University, Beijing 100871, China

Received 2014 December 30; accepted 2015 November 4

**Abstract** The South Galactic Cap $u$-band Sky Survey (SCUSS) was established in 2009 in order to provide a photometric input catalog for target selection of the Large Sky Area Multi-Object Fiber Spectroscopic Telescope (LAMOST) project. SCUSS is an international cooperative project between National Astronomical Observatories, Chinese Academy of Sciences, and Steward Observatory at the University of Arizona, using the 90 inch (2.3 m) Bok telescope on Kitt Peak. The telescope is equipped with a prime focus camera that is composed of a mosaic of four $4096 \times 4096$ CCDs and has a field of view of about 1 deg$^2$. From 2009 to 2013, SCUSS performed a sky survey of an approximately 5000 deg$^2$ field of the South Galactic Cap in $u$ band, including the Galactic anticenter area and the SDSS-IV extended imaging area. The limiting magnitude of SCUSS is deeper than 23 mag (at a signal-to-noise ratio of 5). In this paper, we briefly describe the goals of this project, method of observations and data reduction, and we also introduce current and potential scientific activities related to the SCUSS project.

**Key words:** observation: sky survey — techniques: data reduction — objects: stars and galaxies

## 1 INTRODUCTION

Cosmological models predict that the large scale distribution of galaxies traces the underlying matter density structure, which evolved from density fluctuations imprinted on the cosmic microwave background in the early universe. Galaxy clusters formed in the most overdense areas of this structure. Important constraints on cosmology models can be obtained by measuring large scale galaxy clustering. Statistics of the intrinsic properties of galaxies, including their luminosity, color and morphology, reveal the formation and evolution of the galaxy population across cosmic time. Detailed three dimensional maps of different stellar populations of the Milky Way, determined from multi-color photometric measurements, can strongly constrain the assemblage history of our Galaxy.

In order to make reliable measurements of the large scale distribution of galaxies and stars in the Galaxy, deep, homogeneous sky surveys are necessary. Before the Sloan Digital Sky Survey (SDSS), most optical sky surveys were based on photographic plates. Since 2000, SDSS has made photometric and spectroscopic observations covering about one quarter (14 555 deg$^2$) of whole sky and obtained spectroscopic measurements for nearly 2.6 million stars and galaxies, as well as over 300 000 quasars *(http://www.sdss3.org/dr10)* (Ahn et al. 2014). SDSS data have supported fundamental work from asteroids to cosmology, across an extraordinary range of astronomical disciplines, including the properties of galaxies, the evolution of quasars, the structure and stellar populations of the Milky Way, the dwarf galaxy companions of the Milky Way and M31, asteroids and other small bodies in the solar system, and the large scale structure of the universe (Eisenstein et al. 2011).

The Large Sky Area Multi-Object Fiber Spectroscopic Telescope (LAMOST) is the largest Chinese optical sky survey project (see Su et al. 1998 for the details) to date. Two main scientific programs are included in LAMOST observation plans. They are the LAMOST Extra Galactic Survey (LEGAS) and the LAMOST Experiment for Galactic Understanding and Exploration (LEGUE). The goal of LEGAS is to conduct spectroscopic surveys of galaxies and quasars in the North Galactic Cap and the South Galactic Cap, producing a database of 6 million extragalactic spectra, including low-redshift galaxies as well as quasars at $z = 1 - 3$ and a large sample of low-redshift

active galactic nuclei (AGN). The LEGUE project is addressing the structure of the Galactic halo and disk components. The large stellar spectral database will provide data to substantiate our models of star formation, the formation history of the Galaxy, and the structure of the gravitational potential of the Galaxy. Just as in previous and ongoing optical spectroscopic sky surveys such as SDSS, the candidate targets for LAMOST need to be selected carefully to obtain the maximum number of interesting objects and to minimize selection effects.

The target of SDSS spectra observations are the main galaxy sample (Strauss et al. 2002), luminous red galaxies (Eisenstein et al. 2001) and quasar candidates (Richards et al. 2002). Their color and morphology measured from SDSS images are mainly used for select these objects. By comparing an object profile in the image with the associated PSF, most of the galaxies can be well separated from point sources. For classification of objects, measurement of the spectral energy distribution (SED) from multi-color observations is crucial. Similar methods are used for target selection in LAMOST (Wu & Jia 2010).

A deep photometric survey beyond SDSS is needed for a complete compilation of LAMOST targets. The South Galactic Cap $u$ band Sky Survey (SCUSS) is designed to provide part of this essential input data to LAMOST. SCUSS has been carried out by National Astronomical Observatories, Chinese Academy of Sciences (NAOC) in collaboration with Steward Observatory at the University of Arizona (SO/UA) and Shanghai Astronomical Observatory (SHAO). NAOC provided funding for upgrading the 90Prime instrument to expedite SCUSS and hence meet the needs of the SCUSS project. Steward Observatory collaborated with the SCUSS team and provided telescope time and associated technical resources to support the observations. The original goal of the SCUSS project was to undertake a $u$ band survey of a 3700 deg$^2$ region in the South Galactic Cap defined by Galactic latitude lower than –30° and equatorial declination (DEC) higher than –10°. With 5-minute exposures for a limiting magnitude of 23 mag (AB), the survey would be completed within a period of approximately three years. The technical goals of the project were to upgrade the existing imaging system with new blue-optimized CCDs, to improve the readout noise of the controller, and to enhance the overall operation of the 90Prime instrument and telescope control system. The limiting magnitude of SCUSS is 1.5 mag deeper than that of the SDSS $u$ band and can be calibrated by SDSS in most of the SCUSS fields. When combined with data in other bands ($griz$ etc.) from the SDSS and PanSTARSS, SCUSS will be a valuable data set for a wide range of research areas in Galactic and extragalactic astronomy.

This paper presents an overview of the SCUSS project. In this paper, we will briefly describe the SCUSS project in Section 2 and discuss the data products in Section 3. The scientific goals of the project are outlined in Section 4. Our summary is given in Section 5.

## 2 THE SURVEY

### 2.1 SCUSS Facilities

SCUSS is a $u$ band (354 nm) survey utilizing the 1° field of view (FoV) 90Prime camera, mounted at the prime focus of the Bok 2.3 m (90 inch) telescope, which is located on Kitt Peak, near Tucson, AZ, USA. This telescope has been in operation since 1969 and is managed by Steward Observatory, at the University of Arizona. 90Prime is a prime-focus wide-field camera including a four-element corrector with a modified focal ratio of f/2.98 and a six-position filter wheel (Fig. 1). The CCD array is a mosaic of four $4\mathrm{k} \times 4\mathrm{k}$ STA CCDs, which have been modified for back illumination by the University of Arizona Imaging Technology Laboratory (Fig. 2). It is a blue sensitive CCD camera, specially designed for the SCUSS project, which has an efficiency near 80% in the SDSS $u$ band (Fig. 3). The camera provides an imaging area of 1.0 deg$^2$. The edge-to-edge FoV, including the inter-CCD spacing, is $1.085 \times 1.015$ deg$^2$ with a plate scale of $30.2''$ mm$^{-1}$ or $0.454''$ pixel$^{-1}$. The camera filter wheel can hold up to six filters. The $u$ band filter, which we used in the SCUSS project, is similar to the SDSS $u$ band filter but has a blueward shift of about 24 Å and is slightly narrower than the SDSS $u$ band filter (Fig. 4). A small color item is used in systematic magnitude conversion between the standard SDSS $u$ band and the SCUSS $u$ band photometric system (Zou et al. 2015a). A software package has been developed for controlling the telescope position and camera, allowing the survey observations to be made automatically. The same software also checks the focus of the camera, telescope pointing and evaluates magnitude limit and imaging quality. The status of the observation can then be adjusted in real time based on these measurements.

### 2.2 Strategy Used for SCUSS Observations

We have developed automated software to plan the observing schedule. The program generates the total observation plan adaptively, based on the progress of observations. It assists the observers to produce an automatic observation script every night and optimizes observing efficiency. We separate the SCUSS survey area into different fields appropriate for sizes of the camera FoV. Each field is observed twice with an exposure time of about 2.5 minutes. The field center of the second exposure is shifted from that of the first exposure by 1/2 of the CCD field (about 0.25°). This provides an internal self flux calibration (Fig. 5). We group the fields within the same declination range into several tens of blocks in order for continuous observation without large telescope movement for a duration of about 2 hours. The prioritization of field selection is:

(1) Lower declination blocks. The observation is arranged in direction from lower to higher declination. The lower declination blocks are more difficult to schedule at low airmass for observation.

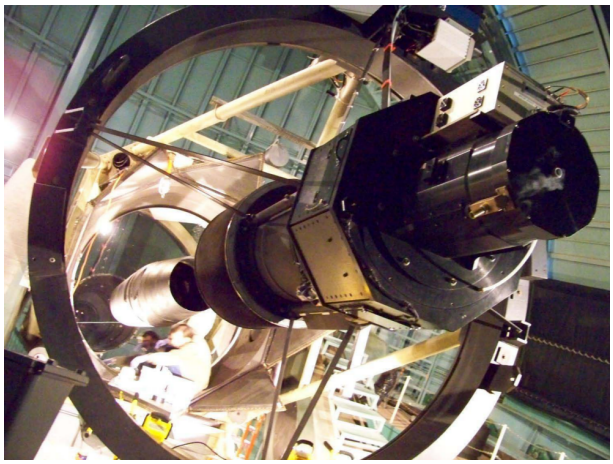

**Fig. 1** The 90Prime camera on the prime focus of the Bok Telescope.

(2) Lowest airmass of the same declination range. For each declination range (3° wide), we select the block with the lowest airmass as fields with the highest observing priority.
(3) Airmass range. The first block of each night is selected if its air mass is smaller than or equal to 1.6; the following block can be selected in case its airmass is smaller than or equal to 1.4.
(4) No backward observation in the right ascension (R.A.) direction. A new observation block is selected along the direction of increasing R.A. so that it can always maintain the fields being observed near the meridian. This has been shown to be important for keeping good telescope pointing and good camera focus due to less dramatic mechanical movements.
(5) The R.A. range of the first block is only observed one time, because only a small number of fields with the lowest R.A. can be observed in September, and we want to leave more field blocks with lower R.A. for other observational nights in September.
(6) All the observed fields are considered in the next new observing schedule so that we can always optimize the new schedule based on the observation history.

The strategy above has all been coded and successfully implemented in SCUSS, with high observing efficiency, optimized airmass coverage, and no dead time because of the lack of targets.

### 2.3 Observation

Based on simulations, we estimated that with 50 clear nights, we will be able to complete all the SCUSS survey area. We scheduled a total of 80 nights to guard against loss due to bad weather and technical issues. Observations for the survey started in September 2009 and ended in November 2013. Usually there were 6–7 scheduled nights in each month from September to December. The mean dark time was about 10 hours per night. Statistically, the weather at Kitt Peak is better in October and November

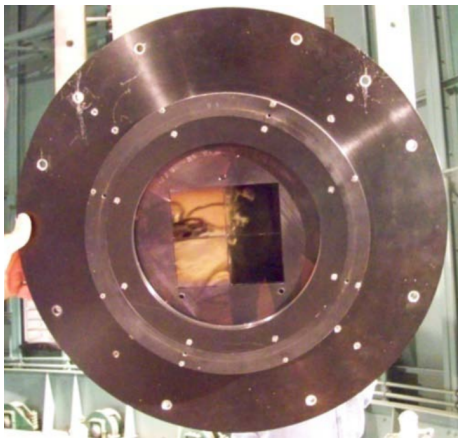

**Fig. 2** The four $4\text{k} \times 4\text{k}$ CCD devices, as seen through the camera dewar window.

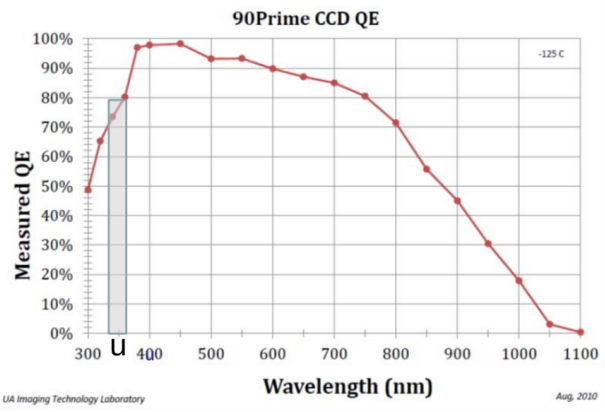


**Fig. 3** The quantum efficiency curve of the CCD. The efficiency in the $u$ band is about 80%.

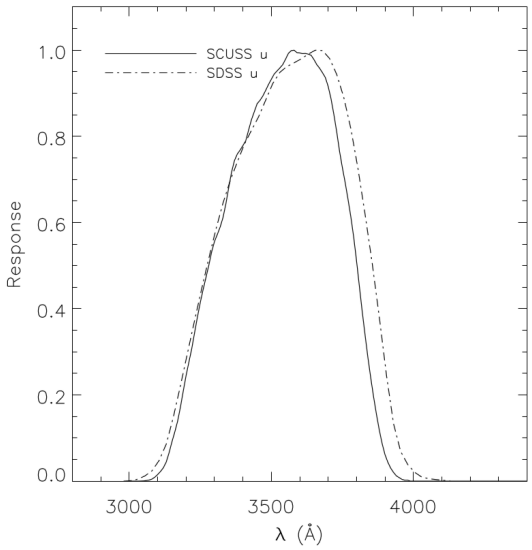


**Fig. 4** Response curves of both the SCUSS $u$ and the SDSS $u$ filters. Both curves include atmospheric extinction at an airmass of 1.3 and are normalized to their maxima. The SCUSS $u$ band filter has a 24 Å blueward shift and is slightly narrower than the SDSS $u$ band filter (Zou et al. 2015a).

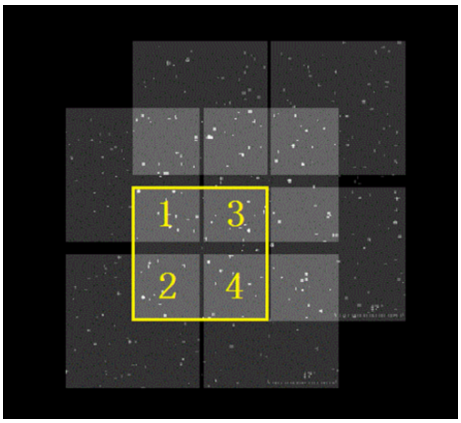


**Fig. 5** Each field is observed twice in a two-point dithering pattern. Each CCD frame can be calibrated by four previous exposure frames and this frame can calibrate four other overlapping frames. Then, all the frames can be internally calibrated.

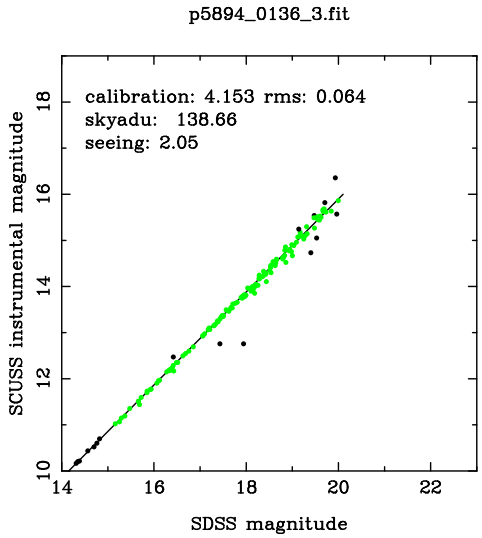


**Fig. 6** The seeing, sky background and magnitude zero point are obtained in real time, based on the last image obtained. The parameters are used to calculate the subsequent exposure time to keep the magnitude limit homogeneous across the survey area.

than other months. The fractions of clear nights were 54%, 69%, 95%, 67% and 64% for months from September to December, respectively, for a period from 2009 to 2013.

Before and after observations on every night, dome flat-field images and bias frames were obtained. Several twilight flats were taken for comparison and checking. Observers checked all the images in real time with tools developed before or during the survey. These tools can estimate the focus of the camera, seeing, atmospheric transparency, and sky background (Fig. 6). These parameters were used for calculating the exposure time for the next exposure or making a repeated exposure of the same field if the image quality did not satisfy the requirement. After each observing run, the data reduction team checked image quality using the photometric catalogs of SDSS. In the non-SDSS survey field, an equivalent catalog from UCAC

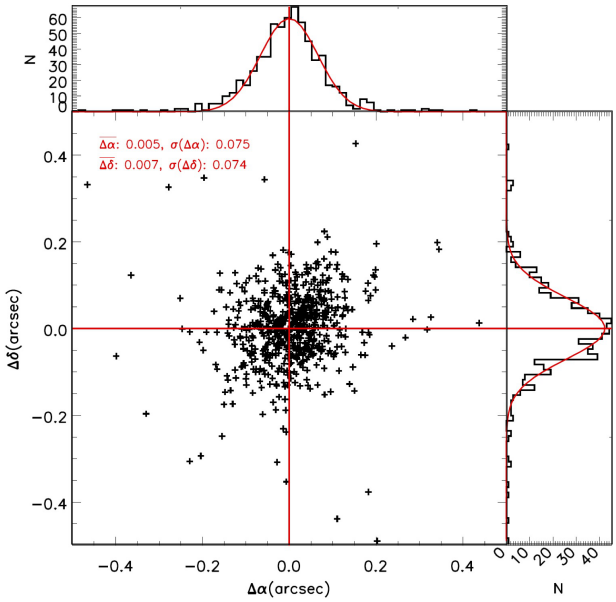


**Fig. 7** The calibrated precision of astrometry is about $0.1''$.

was used. In this way, all the fields with bad quality would be re-observed.

By the end of all the SCUSS observation runs, the total observation area was nearly 5000 deg$^2$, which included 3612 deg$^2$ in the South Galactic Cap region that was originally planned, an extra 475 deg$^2$ in the region that was also covered by the SDSS footprint, and a 690 deg$^2$ area extending to the Galactic anticenter region. The Galactic anticenter area was observed for the LAMOST key project of Galaxy structure and the extra area covered by SDSS is used for target selection in the SDSS-IV Extended Baryon Oscillation Spectroscopic Survey (eBOSS) project (Comparat et al. 2015).

Figures 8 and 9 show the SCUSS sky coverage. The stacked images are shown in these two figures. The grid of equatorial and Galactic coordinates are overplotted in these figures to show the field location of the SCUSS observations.

## 2.4 Data Reduction Pipeline

A data reduction pipeline is specially designed for the SCUSS data, which includes basic image processing, astrometric and photometric calibrations, image stacking and photometry. The detailed description of the pipeline can be found in Zou et al. (2015a). We briefly summarize the pipeline below:

(a) **Raw Image Processing**
This step will detrend the raw images, including corrections for overscan, dark, bias, flat-field and CCD cross-talk.

(b) **Astrometric and Photometric Calibrations**
Astrometric solutions are derived by cross-identifying objects in the science frames with the Fourth US Naval

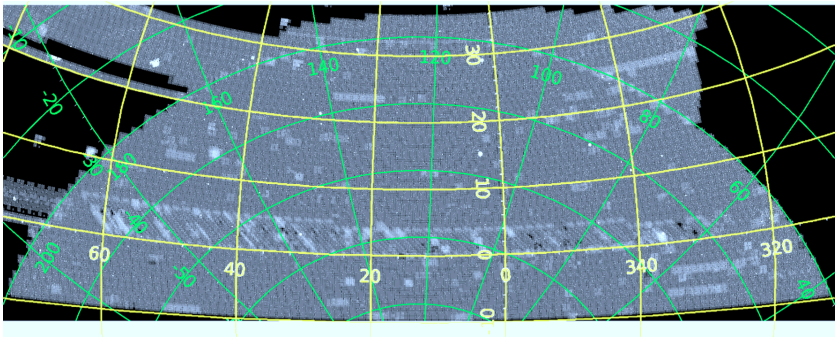


**Fig. 8** A directly combined image that shows the area observed by SCUSS in the South Galactic Cap area and the extended area within the SDSS imaging footprint (*top-right*). The Galactic coordinate grid is shown in green and the equatorial coordinate grid is in yellow.

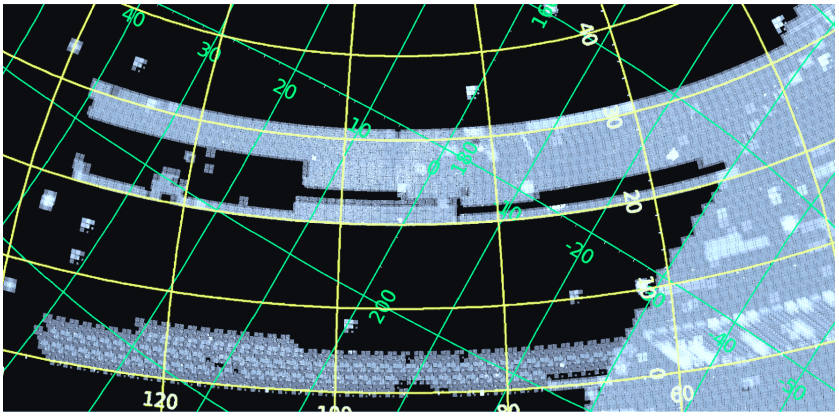


**Fig. 9** Similar to Fig. 8. The directly combined image shows the area observed by SCUSS in the Galactic anticenter region. The Galactic coordinate grid is shown in green and the equatorial coordinate grid is in yellow.

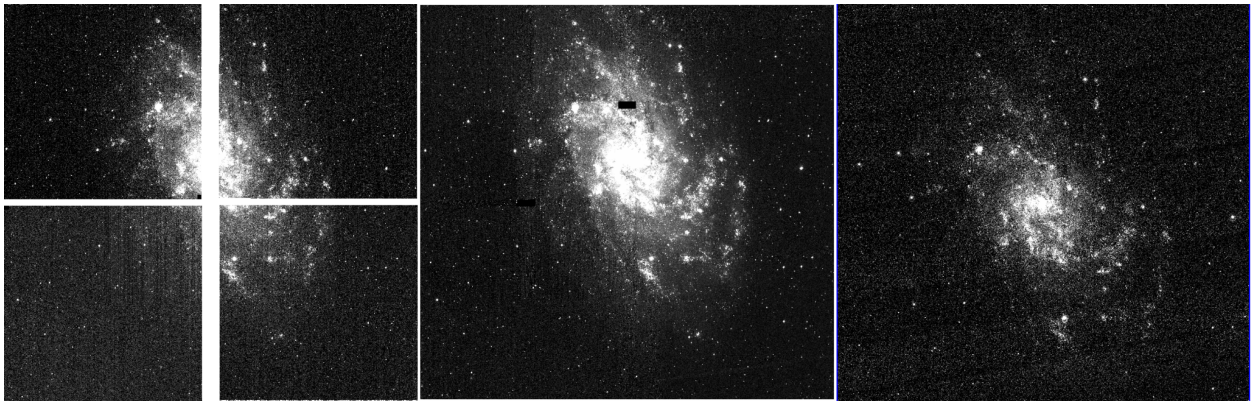

**Fig. 10** An example of a SCUSS single-epoch image (*left*), a similar stacked image (*middle*) and an SDSS $u$ band image (*right*), in the direction of M33.

Observatory CCD Astrograph Catalog (UCAC4). In SCUSS, the total external positional accuracy is about 0.1 arcsec (Fig. 7). The photometric calibration for SCUSS utilizes the photometry of SDSS objects as local standard stars, while for the area not covered by SDSS, we photometrically calibrated the data internally by transferring the photometric solution from overlapping image regions. The SDSS calibrations have recently been improved to a sub-percent precision (Finkbeiner et al. 2014) in photometric calibration. Our filters are very close to SDSS filters with minimal color terms (Zou et al. 2015a).

(c) **Image Stacking**

Imaging quality is first assessed to ensure a homogeneous set of images for each field. Based on the central coordinate of each field, we stack related single-epoch images to form a combined image. We subtract the sky backgrounds from the re-sampled images.

Their photometric zero points are converted to linear flux weights. The remaining signals after removing backgrounds are weighted by these weights and then co-added. Cosmic ray rejection is implemented by a sigma clipping algorithm.

(d) **Photometry**
We carry out photometric measurements on the stacked images. For circular aperture photometry, the core code of aperture photometry in DAOPHOT (Stetson 1987) is used to measure aperture magnitudes. Automatic aperture photometry, generating a so-called automatic magnitude, is performed using SExtractor (Bertin & Arnouts 1996). A code for performing PSF photometry was also developed for the SCUSS project. It takes the PSF profile from SExtractor and performs PSF fitting on the science images. Model photometry with the SDSS morphological parameters in the $r$ band is also calculated to generate consistent model measurements with the SDSS "modelMag." Some of the stacked images have non-homogeneous image quality when they are assembled by a set of single-epoch images observed in different conditions (such as seeing). The above photometric methods are then applied to single-epoch images and measured fluxes are co-added to form co-added photometric magnitudes.

## 3 DATA PRODUCTS

We have well-calibrated single-epoch images and stacked images. Figure 10 shows an example of these images. The SDSS $u$ band image is also shown in this figure as a comparison. Normally, each SCUSS field has two exposures, so the stacked images are twice as deep as the single-epoch images. We apply a wide variety of photometric measurements to the stacked images, including automatic magnitudes with variable apertures, aperture magnitudes, and PSF magnitudes and model magnitudes. We also perform these photometric measurements on single-epoch images and generate co-added magnitudes, including co-added aperture, PSF and model magnitudes. PSF and aperture magnitudes are more suitable for point sources, while model magnitudes are more suitable for galaxies. Automatic magnitudes can be regarded as a universal magnitude for both types of sources.

Figure 11 shows a comparison of color-color diagrams using SCUSS and SDSS $u$ bands. Spectroscopically confirmed stars by SDSS are presented in this figure. The dispersion of $u_{\rm SCUSS} - g_{\rm SDSS}$ is smaller than that of $u_{\rm SDSS} - g_{\rm SDSS}$, especially for faint M stars. There are quite a few stars far away from the star sequence in the left panel. They are targeted as quasar candidates and confirmed as stars. In the right panel showing the deep SCUSS $u$ band, these stars are in the stellar locus due to smaller photometric error. The SCUSS images and related catalogs were recently released to the international astronomical community (Zou 2016). All of the data products can be directly accessed through the Chinese Astronomical Data Center (CAsDC) (*http://explore.china-vo.org*).

## 4 SCIENTIFIC APPLICATIONS OF SCUSS

As one of the SDSS $u$, $g$, $r$, $i$ and $z$ filters, the $u$ band central wavelength is located at 3550 Å, bluer than the 4000 Å break. The 4000 Å break is caused by many hydrogen and metal absorption lines with $\lambda < 4000$ Å in the atmospheres of stars with spectral type later than O and B. Colors that include $u$ band measurements are more sensitive to stellar temperature, surface gravity and metallicity than the other optical filter bands since they sample below the 4000 Å break and they are very useful for photometrically classifying both stars and galaxies. Early-type galaxies have a strong 4000 Å break. Late type spirals have a weak break and the irregulars have little or no 4000 Å break. The $u$ band is the most important optical filter band to select AGN or quasar targets using color-color diagrams (Richards et al. 2002). As a filter in near ultraviolet (NUV), the $u$ band morphological behaviors in the images are very similar to those in the UV bands (Kuchinski et al. 2000) and are most sensitive to recent or ongoing star formation.

The SCUSS survey makes two repeated exposures in every sky area during a short time interval. It is expected to find some candidates of short period variables. In the overlapping sky field of SDSS and SCUSS surveys, we can find many long term variable objects including quasars/AGN, supernovae and all kinds of variable stars.

Figure 12 gives an example of a variable object discovered in SCUSS and SDSS images.

### 4.1 Extra Galactic Astronomy and Cosmology

From early to late type galaxies in the Hubble type sequence, most of them show late type structure in UV (Kuchinski et al. 2000). From $u$ band images, the profiles of galaxies are much more similar to those of UV in comparison with other optical bands.

Figure 13 presents a comparison of imaging between GALEX NUV and SCUSS $u$ band images of NGC 3351. The SCUSS image shows similar structures as the GALEX image but is deeper in terms of magnitude limit and has a higher spatial resolution than the GALEX image. The $u$ band image traces the location of OB stars in the star forming region. The spiral arms, bars and rings in the galaxies are much more prominent than in the other optical bands. The morphological types of the galaxies shown in the $u$ band may be different from those shown in other optical bands, especially for late type galaxies, because $u$ band images have a higher contrast for showing galaxy structure. It is possible to perform a new morphological classification based on the $u$ band images. This new classification will be important for studying the structure and evolution history of galaxies.

The $u$ band magnitude is also very important in estimating photometric redshift of nearby galaxies (Ilbert et al. 2006). In the BATC project, more than 30 nearby galaxy

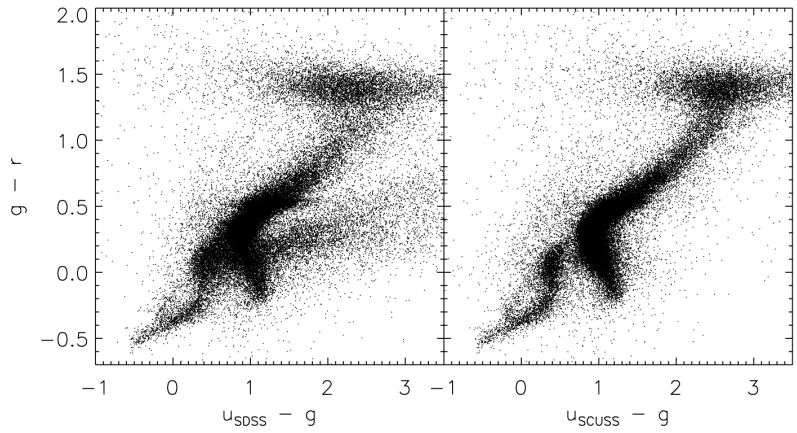


**Fig. 11** Color-color diagrams of spectroscopically identified stars in SDSS. The left panel is the diagram made with the SDSS $u$ band while the right panel is made with the SCUSS $u$ band.

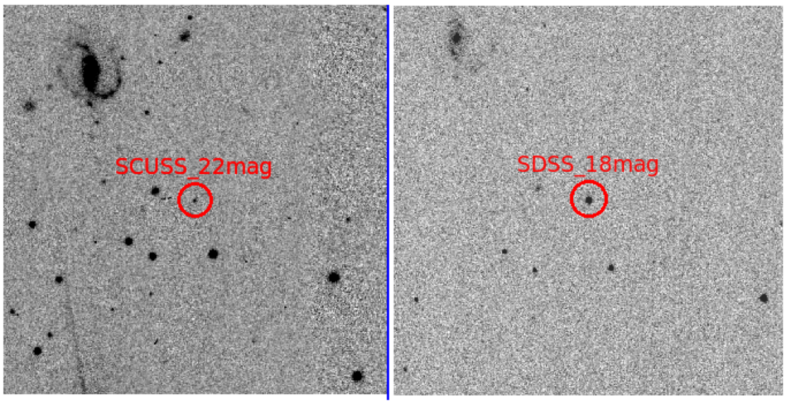


**Fig. 12** A variable (22:40:24.54, +03:10:36.00, 2000.0) shows its variation of about 4 mag between SCUSS (*left*) and SDSS (*right*) images.

clusters were observed in 15 colors with a magnitude limit of ∼20 in AB (Tian et al. 2012). The SCUSS data include most of these galaxy clusters. The SCUSS $u$ band data will significantly improve the quality of the photometric redshift estimation of nearby galaxies ($z < 1$) and member galaxies in the galaxy clusters will be better selected.

The baryon acoustic oscillation (BAO) feature in the power spectrum of galaxies provides a standard ruler to probe the accelerated expansion of the Universe. Current surveys (e.g., SDSS) covering a co-moving volume sufficient to unveil the BAO scale are limited to redshift $z = 0.7$. We are now studying several galaxy selection schemes aiming at building an emission-line galaxy (ELG) sample in the redshift range $0.6 < z < 1.0$. That would be suitable for future cosmological studies by using the spectroscopic data from eBOSS. The SCUSS data are being used for target selection of ELGs in the eBOSS project, associated with SDSS-IV, and have potential abilities for selecting other types of the objects, including low-redshift quasars.

One of the main science goals of SCUSS is to select quasar candidates for the LAMOST project. Quasar selection before SDSS DR10 was mainly based on SDSS optical colors. For redshift $z < 2.2$ or $z > 3.3$, quasars can be easily selected due to their UV excess and emission lines. The $u$ band is crucial for selecting such quasars and dramatically improves targeting efficiency. Most of the SCUSS area is covered by the SDSS imaging survey and the SCUSS $u$ band is about 1.5 mag deeper than SDSS. The SCUSS $u$ band data, together with other SDSS bands, will greatly improve quasar selection. In addition, quasar variability between the SCUSS and SDSS $u$ band observations is much larger than that of stars (see Fig. 13). This can be used to select quasars in the redshift range of $2.2 < z < 3.0$, where optical colors of quasars are similar to those of stars (see Fig. 14).

The $u$ band luminosity of a galaxy is proportional to the total mass of short-lived massive OB stars and therefore to the star formation rate (SFR), when the galactic extinction is corrected. However besides SDSS, there are very few large field $u$ band surveys. Baldry et al. (2005) analyzed the SDSS $u$ band selected galaxies and derived the $u$ band luminosity function down to an absolute magnitude of –15 mag. They found that the faint-end slope at low-

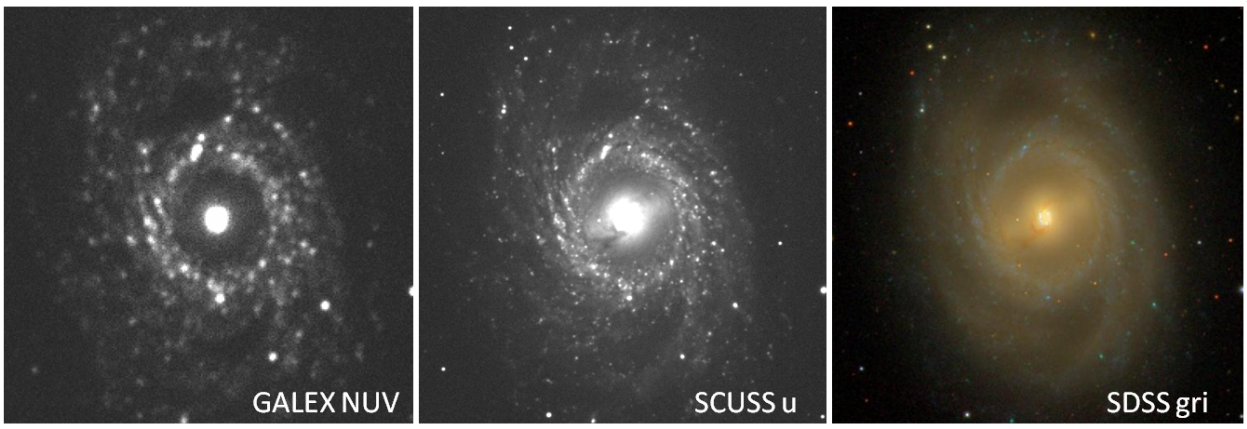


**Fig. 13** The images of the GALEX NUV band (*left*), SCUSS $u$ band (*middle*) and a color image from SDSS composed of $g$, $r$ and $i$ bands (*right*). The SCUSS image shows more similar structure to the GALEX image in UV but is deeper in terms of magnitude limit and has higher spatial resolution than the GALEX image.

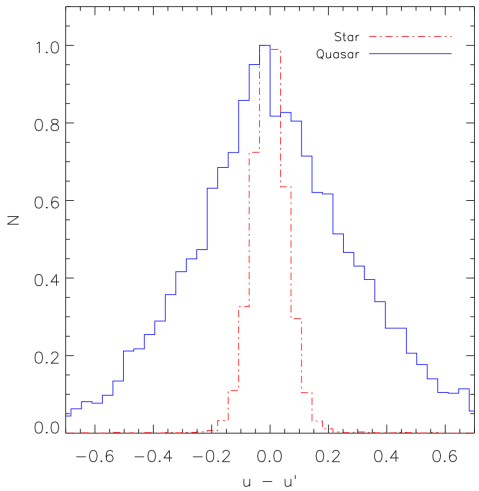


**Fig. 14** Distributions of the magnitude differences between SCUSS and SDSS for quasars (*solid line*) and stars (*dot-dashed line*), which are normalized to their maxima. The SCUSS $u$ and SDSS $u'$ magnitude errors are limited to be less than 0.05 mag (Zou et al. 2015b).

redshift is nearly flat. With our SCUSS data, we can investigate the $u$ band luminosity function at 1.5 mag fainter than previous work. In particular, we will combine our SCUSS catalog with the redshift available from the BOSS survey (Eisenstein et al. 2012), and explore star formation in massive galaxies at $z < 0.6$.

The $u$ band luminosity is also more sensitive to stellar age, metallicity and interstellar extinction of nearby galaxies than other optical filter bands because it is located in the UV side of the 4000 Å break. Therefore, the $u$ data are the most important band in mapping the optical SED for analyzing the stellar population of nearby galaxies (Fritze-v. Alvensleben et al. 2006). The SCUSS $u$ band data, together with data from other present or future sky survey projects, are highly valuable in understanding galaxy formation and evolution, and structure of the universe.

Compared to optical images, the UV images of the galaxies usually show less prominent bulges and galaxy light appears to be more patchy with distinct star formation regions (O'Connell 1997; O'Connell & Marcum 1996). The UV appearance mainly traces the distribution of young stars. Therefore, integrations of the $u$ band luminosity are entirely below 4000 Å. So $u$ band strongly constrains the total mass of short lived OB stars and can be used for estimating the star formation rate SFR of the galaxies (Lilly et al. 1996; Madau et al. 1998; Cowie et al. 1999; Wilson et al. 2002; Hopkins et al. 2003; Baldry et al. 2005). For higher redshift galaxies with $z \leq 2$ which have statistically higher SFR (Kurczynski et al. 2012; Madau et al. 1998), the Lyman alpha emission feature is redshifted into $u$ band, allowing selection of high-redshift star forming galaxies.

### 4.2 Structure of the Galaxy and Its Stellar Components

With a magnitude limit deeper than 23 mag, most objects in the image are external galaxies. These objects are the background sources of the Milky Way. The intrinsic color of galaxies and the mean color index that include the SCUSS $u$ band can be used for determination of an interstellar

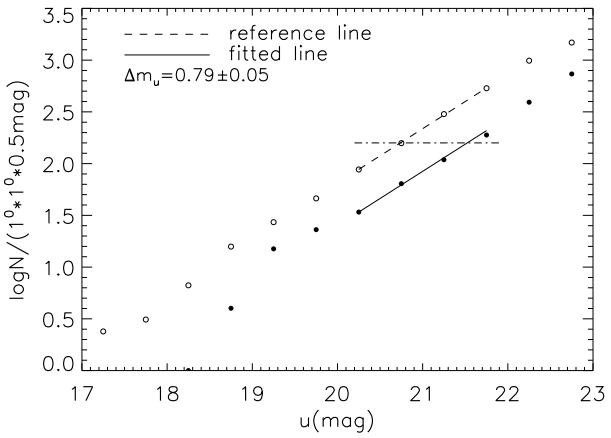


**Fig. 15** The galaxy number counts in two selected SCUSS fields. The two fields are located at ($l = 113.35$, $b = -60.5$, *open circles*) and ($l = 93.68$, $b = -33.50$, *solid circles*), respectively. The dashed and solid lines show the fitting relation $N(m) \propto 10^{0.6m}$ of the number counts for each fields. The dot-dashed line represents the shift between the two fitting lines, showing an extra dimming of 0.79 mag.

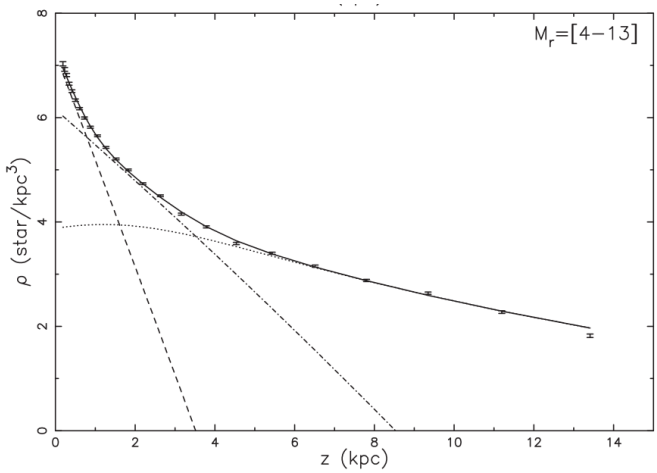


**Fig. 16** SCUSS observed (*dots with error bars*) and best-fit (*solid line*) space density functions for the considered Galaxy population components (Jia et al. 2014).

extinction map of our Galaxy in the South Galactic Cap region. Similar methods, e.g., the synthetic field method, have also been used for studying the extinction of nearby galaxies (González et al. 1998; Mörtsell 2013).

Figure 15 shows an example of galaxy number count in two selected fields. According to the SFD Galactic extinction map (Schlegel et al. 1998), values for Galactic extinction in $u$ band in these two fields are $A_u = 0.095$ and $A_u = 0.79$, respectively. Due to the large extinction coefficient in $u$ band, the values of $A_u$ in these two fields show big differences although they are both in regions with high Galactic latitude. Using the SCUSS photometric catalog, we are now conducting a detailed study of the Galactic extinction with galaxy number counts (Li et al., in preparation).

A star counting method can be used to study our Galaxy. Many previous works studied the size of the thin disk, thick disk and bulge of the Galaxy (Du et al. 2006, 2008). Using SEDs from multi-color photometric observations, main sequence stars are selected, then the photometric distance to the stars can obtained from comparison of the apparent magnitude and intrinsic absolute magnitude. Based on the SDSS and SCUSS early data, we use a star count method to estimate Galactic structure parameters at intermediate Galactic latitude with 10 180 main sequence stars in an absolute magnitude interval of $4 \leq M_r \leq 13$ (Jia et al. 2014), and estimate the Galactic structure parameters in each absolute magnitude interval to explore their possible variation with absolute magnitude.

Our study shows that the parameters depend on absolute magnitude (Fig. 16).

As special type of star, blue horizontal branch (BHB) stars are excellent tracers of Galactic halo structure because they are luminous and have a nearly constant absolute magnitude within a restricted color range. With an extra 1.5 mag depth compared to SDSS, SCUSS plays a cru-

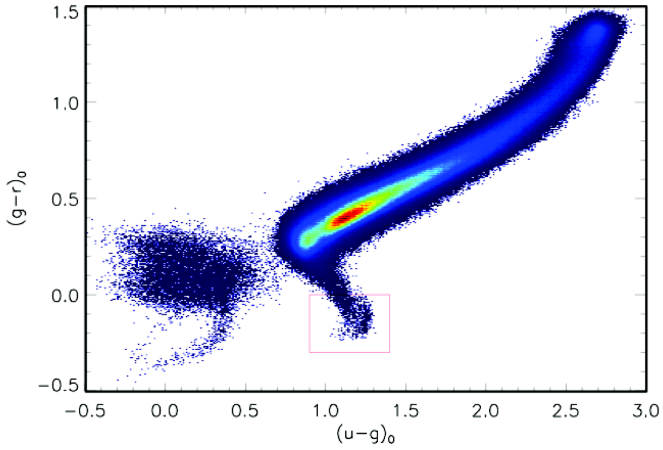


**Fig. 17** The distribution of BHB stars in the color-color diagram with SCUSS $u$ band and SDSS $g$ and $r$ band (Nie et al. 2015).

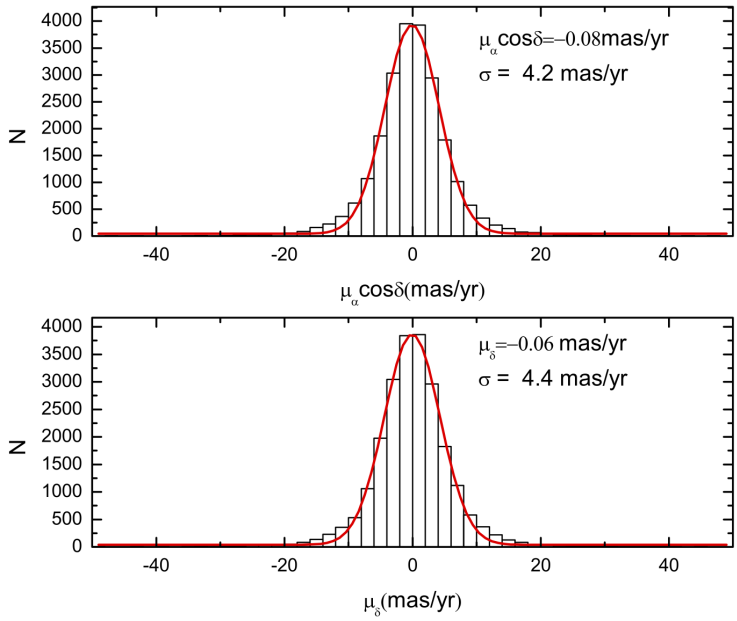


**Fig. 18** The proper motion distributions of quasars in the SCUSS catalog in right ascension $\mu_\alpha \cos\delta$ (*top panel*) and in declination $\mu_\delta$ (*bottom panel*). Only quasars whose proper motions with absolute value less than 50 mas yr$^{-1}$ in each component are used to fit the Gaussian function. The red solid line in each panel is the best-fitting Gaussian function. The best-fitting parameters of the Gaussian function with the associated mean and the dispersion are also labeled in each panel.

cial role in halo substructure detection because it provides us a much larger volume of the outer halo. SCUSS+SDSS selected BHB stars can trace the outer halo to as far as 120 kpc. We combined SCUSS $u$ band with SDSS DR9 single epoch $g$ and $r$ photometric bands to detect BHB stars and explore substructures in the outer halo (Nie et al. 2015).

Figure 17 shows the $(u-g)$ vs $(g-r)$ color-color diagram for all the objects from a SCUSS/SDSS overlapping region with $16 < u_{\rm scuss} < 21, u_{\rm err}, g_{\rm err}, r_{\rm err} < 0.3$ mag. Since BHB stars are A-type stars, they are located in the region defined by $0.9 < u-g < 1.4, -0.3 < g-r < 0$ (Yanny et al. 2000; Sirko et al. 2004; Deason et al. 2011), as shown by the red box in Figure 17.

A catalog of proper motions using the International Celestial Reference System (ICRS), with highly precise positions and proper motions and deep magnitude limits, provides highly valuable information on Galactic structure, Galactic kinematics and stellar populations. Most sky fields of SCUSS were imaged twice in the course of the survey from 2010 to 2013, and proper motions of stars can be derived precisely using the SCUSS data and the earlier Guide Star Catalog-II (GSC-II) Schmidt plate data. The GSC-II Schmidt plate dataset is an all-sky astrophotometric database derived from the digitization of the Palomar and UK Schmidt surveys. The large time interval between SCUSS (2010–2013) and GSC-II (1950–2000) will reduce the systematic and random errors of the de-

rived proper motions. The proper motions of quasars can be used to derive the systematic and random errors of the proper motion catalog.

Figure 18 displays histograms of the proper motions in right ascension $\mu_\alpha \cos\delta$ (top) and in declination $\mu_\delta$ (bottom) for all spectroscopically confirmed quasars in the SCUSS proper motion catalog. The random errors of the proper motions are 4.2 and 4.4 mas yr$^{-1}$ in $\mu_\alpha \cos\delta$ and $\mu_\delta$, respectively. The systematic error of $\mu_\alpha \cos\delta$ is about $-0.08$ mas yr$^{-1}$ and the systematic error of $\mu_\delta$ is about 0.06 mas yr$^{-1}$. Our method of calculating absolute proper motions successfully removes the position, magnitude and color dependence on the systematic error of proper motions (Peng et al. 2015).

## 5 SUMMARY

For target selection of LAMOST and related scientific research, we carried out the South Galactic Cap $u$-band Sky Survey (SCUSS) with the 2.3 m Bok telescope and its new blue sensitive CCD camera. The special observation strategy was designed for maximizing the observation time without dead time and for taking internal self-calibrations. New software was developed to control the observation that keeps image quality homogeneous, including frequently checking and adjusting the focus, centering the FoV, correcting the telescope pointing in real time, and estimating the exposure time by calculating the magnitude limit. With 90 effective observing nights during the 105 nights of allocated time spread over 15 runs from September 2009 to December 2013, we have finished a total survey area of about 5000 deg$^2$, not only including the South Galactic Cap area, but also the Galactic anticenter area and an extended SDSS footprint area. The data reduction pipeline was developed for astrometry, flux calibration and photometry. A number of different types of photometric magnitudes were obtained that include aperture magnitude, and PSF and model fitting magnitudes for point and small extended sources in the images. The magnitude ($5\sigma$) is about 23.2 for the PSF magnitude of point sources. By combining the SDSS, WISE and other wide-field sky surveys, the potential legacy value of our SCUSS data both in and beyond Galactic astronomy is immense. SCUSS can be expected to make important contributions in studies of star and galaxy formation and evolution, structure, stellar population and extinction of our Galaxy, variations of AGN, QSOs and stars and many other fields.

**Acknowledgements** The SCUSS project is funded by the Main Direction Program of Knowledge Innovation of Chinese Academy of Sciences (No. KJCX2-EW-T06) and supported by the National Natural Science Foundation of China (NSFC; Nos. 11433005, 11373035, 11203034, 11203031, 11303038 and 11303043), the National Basic Research Program of China (973 Program, Nos. 2014CB845704, 2014CB845702 and 2013CB834902), and the joint fund of Astronomy of the National Natural Science Foundation of China and the Chinese Academy of Science (Grant U1231113). It is also an international cooperative project between National Astronomical Observatories, Chinese Academy of Sciences and Steward Observatory, University of Arizona, USA. Technical support and observational assistance of the Bok telescope are provided by Steward Observatory. The project is managed by the National Astronomical Observatories, Chinese Academy of Sciences and Shanghai Astronomical Observatory. The management and publication of data are supported by the Chinese Astronomical Data Center and the China-VO team.

## References

Ahn, C. P., Alexandroff, R., Allende Prieto, C., et al. 2014, ApJS, 211, 17
Baldry, I. K., Glazebrook, K., Budavári, T., et al. 2005, MNRAS, 358, 441
Bertin, E., & Arnouts, S. 1996, A&AS, 117, 393
Comparat, J., Richard, J., Kneib, J.-P., et al. 2015, A&A, 575, A40
Cowie, L. L., Songaila, A., & Barger, A. J. 1999, AJ, 118, 603
Deason, A. J., Belokurov, V., & Evans, N. W. 2011, MNRAS, 416, 2903
Du, C.-H., Wu, Z.-Y., Ma, J., & Zhou, X. 2008, ChJAA (Chin. J. Astron. Astrophys.), 8, 566
Du, C., Ma, J., Wu, Z., & Zhou, X. 2006, MNRAS, 372, 1304
Eisenstein, D. J., Annis, J., Gunn, J. E., et al. 2001, AJ, 122, 2267
Eisenstein, D. J., Weinberg, D. H., Agol, E., et al. 2011, AJ, 142, 72
Finkbeiner, D. P., Schlafly, E., & Green, G. 2014, in American Astronomical Society Meeting Abstracts, 223, #116.14
Fritze-v. Alvensleben, U., Papaderos, P., Anders, P., et al. 2006, in IAU Symposium, 232, The Scientific Requirements for Extremely Large Telescopes, eds. P. Whitelock, M. Dennefeld, & B. Leibundgut, 241
González, R. A., Allen, R. J., Dirsch, B., et al. 1998, ApJ, 506, 152
Hopkins, A. M., Miller, C. J., Nichol, R. C., et al. 2003, ApJ, 599, 971
Ilbert, O., Arnouts, S., McCracken, H. J., et al. 2006, A&A, 457, 841
Jia, Y., Du, C., Wu, Z., et al. 2014, MNRAS, 441, 503
Kuchinski, L. E., Freedman, W. L., Madore, B. F., et al. 2000, ApJS, 131, 441
Kurczynski, P., Gawiser, E., Huynh, M., et al. 2012, ApJ, 750, 117
Lilly, S. J., Le Fevre, O., Hammer, F., & Crampton, D. 1996, ApJ, 460, L1
Madau, P., Pozzetti, L., & Dickinson, M. 1998, ApJ, 498, 106
Mörtsell, E. 2013, A&A, 550, A80

Nie, J. D., Smith, M. C., Belokurov, V., et al. 2015, ApJ, 810, 153
O'Connell, R. W., & Marcum, P. 1996, astro-ph/9609101
O'Connell, R. W. 1997, in American Institute of Physics Conference Series, 408, ed. W. H. Waller, 11
Peng, X. Y., Qi, Z. X., Wu, Z. Y., et al. 2015, PASP, 127, 250
Richards, G. T., Fan, X., Newberg, H. J., et al. 2002, AJ, 123, 2945
Schlegel, D. J., Finkbeiner, D. P., & Davis, M. 1998, ApJ, 500, 525
Sirko, E., Goodman, J., Knapp, G. R., et al. 2004, AJ, 127, 899
Stetson, P. B. 1987, PASP, 99, 191
Strauss, M. A., Weinberg, D. H., Lupton, R. H., et al. 2002, AJ, 124, 1810
Su, D. Q., Cui, X., Wang, Y., & Yao, Z. 1998, in Society of Photo-Optical Instrumentation Engineers (SPIE) Conference Series, 3352, Advanced Technology Optical/IR Telescopes VI, ed. L. M. Stepp, 76
Tian, J.-T., Yuan, Q.-R., Zhou, X., et al. 2012, RAA (Research in Astronomy and Astrophysics), 12, 1381
Wilson, G., Cowie, L. L., Barger, A. J., & Burke, D. J. 2002, AJ, 124, 1258
Wu, X.-B., & Jia, Z. 2010, MNRAS, 406, 1583
Yanny, B., Newberg, H. J., Kent, S., et al. 2000, ApJ, 540, 825
Zou, H., Jiang, Z. J., Zhou, X., et al. 2015, AJ, 150, 104
Zou, H., Wu, X. B., Wang, S., et al. 2015, PASP, 127, 94
Zou, H., Zhou, X., Jiang, Z. J., et al. 2016, AJ, 151, 37